

# Enhanced Cellular Entry and Efficacy of Tat Conjugates by Rational Design of the Auxiliary Segment

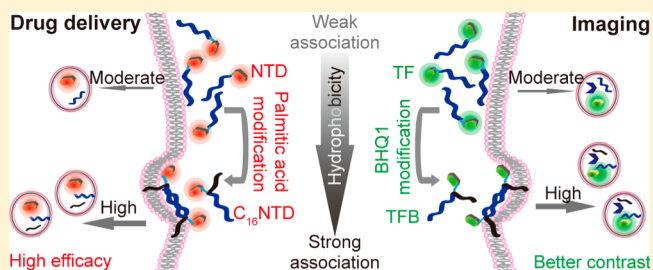
Pengcheng Zhang, Lye Lin Lock, Andrew G. Cheetham, and Honggang Cui\*

Department of Chemical and Biomolecular Engineering and Institute for NanoBioTechnology, Johns Hopkins University, Baltimore, Maryland 21218, United States

**S** Supporting Information

**ABSTRACT:** Conjugation with a cell penetrating peptide such as Tat presents an effective approach to improve the intracellular accumulation of molecules with low membrane permeability. This strategy, however, leads to a reduced cellular entry of molecules that can cross cell membrane effectively. We report here that covalent linkage of an additional hydrophobic unit that mimics a hydrophobic domain near the Tat sequence can further improve the cellular uptake of the parental conjugate into cancer cells regardless of the membrane permeability of the unconjugated molecule. Both fluorescent imaging and flow cytometry measurements confirmed the effect of palmitoylation on the increased internalization of the Tat conjugates with either 5-carboxyfluorescein (5-FAM), a nonmembrane penetrating dye, or doxorubicin, an anticancer cancer drug that can readily diffuse across cell membranes. In the case of the Tat–doxorubicin conjugate, palmitoylation improves the conjugate’s anticancer activity in both drug sensitive and resistant cervical cancer cell lines. We further demonstrate that modification of a Tat–5-FAM conjugate with a hydrophobic quencher could not only efficiently quench the fluorescence outside of cancer cell but also facilitate its entry into MCF-7 breast cancer cells. These results highlight the importance of rational molecular design of using peptide conjugation chemistry in cancer therapeutics and diagnostics.

**KEYWORDS:** cell penetrating peptide, nanobeacon, multidrug resistant, cellular uptake



## INTRODUCTION

Therapeutic or diagnostic agents with intracellular targets must gain access into cells to produce the desired biological effects. The importance of cellular internalization is highlighted by the observation that ~50% of known drug targets<sup>1</sup> and almost all oligonucleotides’ targets are located in the cells.<sup>2</sup> In the particular case of cancer treatments, almost all the targets (DNA, enzymes, cytoskeletons, hormone receptors, etc.) of approved chemotherapeutics and all the potential targets for cancer gene therapy are found within the cells.<sup>3</sup> However, a large portion of therapeutic agents do not possess the ability to effectively cross cell membranes, or have difficulties reaching a therapeutic dose within cells due to various drug resistance mechanisms. For instance, peptides, proteins and oligonucleotides are known to have low membrane permeability, and as a result they are considered to be of limited therapeutic value unless this issue can be addressed.<sup>4</sup> Some small molecule drug candidates, for a number of reasons, also lack the ability to attain sufficient intracellular accumulation.<sup>5</sup> There is also an increasing interest in monitoring disease-related dynamic changes in intracellular signaling, regulation and metabolism networks, for the altered expression levels of intracellular biomacromolecules in cancer cells relative to normal cells could be targets for potential disease prevention, diagnosis and treatment.<sup>6,7</sup> Therefore, it is important and necessary to design

strategies to improve the intracellular accumulation of molecules to reach the desired therapeutic levels.

Several versatile methods have been developed to increase the intracellular accumulation of cargoes, including electroporation,<sup>8</sup> microfluidics,<sup>9</sup> nanocarrier encapsulation<sup>10–14</sup> and conjugation<sup>15–17</sup> and cell penetrating peptide (CPP) modification.<sup>4</sup> Among these approaches, CPP modification shows the broadest application with its ability to aid the intracellular delivery of cargoes ranging from small molecules to nanoparticles both *in vitro* and *in vivo*.<sup>18</sup> The HIV-derived Tat<sub>48–60</sub> peptide (GRK<sub>2</sub>R<sub>2</sub>QR<sub>3</sub>P<sub>2</sub>Q from Tat protein)<sup>19</sup> is one of the most investigated CPPs, and has been conjugated to many different types of cargoes (e.g., nanoparticles) to enhance their intracellular accumulation since its discovery.<sup>20,21</sup> However, we recently found that the intracellular accumulation of doxorubicin, an anticancer drug with reasonably good cell membrane permeability, was actually reduced in a significant way in drug-sensitive cells upon conjugation to Tat peptide, although advantages were observed in drug-resistant cells.<sup>22</sup> Similar observations have been reported when comparing cellular

**Received:** October 23, 2013

**Revised:** December 20, 2013

**Accepted:** January 17, 2014

**Published:** January 17, 2014

uptake of doxorubicin and doxorubicin conjugates on other drug-sensitive cell lines.<sup>23</sup>

The interaction between Tat conjugates and targeting cell surface is apparently crucial for the cellular entry. It is widely accepted that the internalization of Tat (or Tat cargoes) is initialized through electrostatic interactions with cell membrane components such as heparan sulfate proteoglycans<sup>24</sup> and involves cytoskeleton rearrangement during internalization.<sup>25</sup> However, our recent work on Tat conjugates containing different chemical moieties confirms that factors other than electrostatic interactions must also contribute to the cell penetrating efficiency.<sup>22,26,27</sup> Indeed, there have been several reports in the literature on the effect of amphiphilic or hydrophobic peptide sequences and lipid modification to (PRR)<sub>3</sub>,<sup>28</sup> octaarginine (R8),<sup>29,30</sup> peptide analogues,<sup>31</sup> peptide amphiphiles<sup>32,33</sup> and other CPPs<sup>34,35</sup> on their intracellular delivery efficiency of poor cell penetrating molecules. A recent finding suggested the hydrophobic domain of the Tat protein (a36–47) could complex with lipid post its encounter with lipid bilayer,<sup>36</sup> further highlighting the importance of hydrophobic interaction during cellular entry. In this manuscript, we report that palmitoylation to Tat conjugates facilitates efficient intracellular accumulation of the parental molecule, and eliminates the difference in intracellular accumulation and efficacy of doxorubicin due to cancer cell heterogeneity. More importantly, we further demonstrate the extension of the palmitoylation strategy to the design of molecular beacon for intracellular enzyme detection by replacing the palmitoyl tail with a hydrophobic quencher.

## MATERIALS AND METHODS

**Materials.** All Fmoc amino acids were purchased from Advanced Automated Peptide Protein Technologies (AAPP-TEC, Louisville, KY, USA), and Rink Amide MBHA and Wang resins were purchased from Novabiochem (San Diego, CA). 5-Carboxyfluorescein (5-FAM) was purchased from AnaSpec, Inc. (Fremont, CA). Vinblastine and doxorubicin (Dox) were purchased from Avachem Scientific LLC (San Antonio, TX). Palmitic acid was obtained from Sigma-Aldrich (St. Louis, MO). 3-Maleimidopropionic acid was purchased from Bachem (Torrance, CA). All other reagents were of analytical grade and used as received without further purification. C<sub>8</sub>-Tat, NTF, TF, TFB and NTD were synthesized and characterized as we reported previously.<sup>22,26</sup>

**Cell Culture.** MCF-7 breast cancer cells were kindly provided by Dr. Wirtz (Department of Chemical and Biomolecular Engineering, Johns Hopkins University). KB-3-1 and KB-V1 cervical cancer cells were gifted by Dr. Gottesman (Center for Cancer Research, National Cancer Institute). All the cells were grown in DMEM (Invitrogen) containing 10% fetal bovine serum (FBS, Invitrogen) and 1% of antibiotics (Invitrogen) at 37 °C in a humidified incubator (OASIS 6300, CARON, OH) with a 5% CO<sub>2</sub> atmosphere. For KB-V1 cells, 1 μg/mL of vinblastine was added to maintain its multidrug resistance.

**Tat Conjugate Synthesis and Characterization.** All peptide conjugates were synthesized using standard 9-fluorenylmethoxycarbonyl (Fmoc) solid phase synthesis techniques. For C<sub>16</sub>NTF and palmitic acid modified cleavable Tat–doxorubicin conjugate (C<sub>16</sub>NTD), Fmoc-CGRK<sub>2</sub>R<sub>2</sub>QR<sub>3</sub>P<sub>2</sub>Q-Rink, Fmoc-K(Mtt)CGRK<sub>2</sub>R<sub>2</sub>QR<sub>3</sub>P<sub>2</sub>Q-Rink and maleimide modified enzyme degradable peptide–drug conjugates (Mal-GFLG-Dox) were synthesized according

to our previous report.<sup>22</sup> For C<sub>16</sub>NTF, Mtt deprotections were carried out using a mixture of TFA/TIS/DCM with a ratio of 3:5:92 for 5 min, repeating twice, and then the Lys ε-amine was reacted with C<sub>16</sub>/HBTU/DIEA at a ratio of 4:4:6 relative to the peptide, shaking overnight at room temperature. 5-FAM was manually coupled at the peptide N-terminus (after Fmoc removal) with 5-FAM/HBTU/DIEA at a ratio of 4:4:6 relative to the peptide, shaking overnight at room temperature. For C<sub>16</sub>NTD, the N-terminal of the peptide was reacted with C<sub>16</sub>/HBTU/DIEA at a ratio of 4:4:6 relative to the peptide, shaking overnight at room temperature. Mal-GFLG-Dox was then reacted with Ac-C(C<sub>16</sub>)GRK<sub>2</sub>R<sub>2</sub>QR<sub>3</sub>P<sub>2</sub>Q-NH<sub>2</sub> to obtain C<sub>16</sub>NTD according to the procedure described in our previous work.<sup>22</sup> The two conjugates were purified by preparative RP-HPLC using a Varian ProStar model 325 HPLC (Agilent Technologies, Santa Clara, CA) equipped with a fraction collector. Separations were performed using a Varian PLRP-S column (100 Å, 10 μm, 150 × 25 mm) monitoring at 480 nm. Collected fractions were analyzed by ESI-MS (LDQ Deca ion-trap mass spectrometer, Thermo Finnigan, USA) and those containing the target molecules only were combined and lyophilized (FreeZone –105 °C, Labconco, Kansas City, MO), and then stored at –30 °C. The purity of two conjugates was determined by analytical HPLC using the same method we described before.<sup>22</sup>

**Circular Dichroism (CD) Measurement.** The CD spectra of TF, TFB, NTF, C<sub>16</sub>NTF, NTD and C<sub>16</sub>NTD (50 μM in Dulbecco's phosphate-buffered saline, DPBS) were recorded on a J-710 spectropolarimeter (JASCO, Easton, MD) from 195 to 260 nm, and the signal was converted from ellipticity (mdeg) to mean molar ellipticity per residue (deg·cm<sup>2</sup>·dmol<sup>–1</sup>·residue<sup>–1</sup>).

**Cellular Uptake.** MCF-7, KB-3-1 or KB-V1 cells were seeded onto a 24-well plate at 1 × 10<sup>5</sup> cells/well and incubated overnight. The media were replaced with fresh media containing free fluorophore (5-FAM), free drug (Dox), or conjugates (TF, TFB, NTF, C<sub>16</sub>NTF, NTD and C<sub>16</sub>NTD) at a concentration of 5 μM and were incubated with cells for 2 h. If necessary, caprylic acid modified Tat (C<sub>8</sub>-Tat) of various concentrations was added to evaluate the effect of free Tat peptide on the internalization of tested conjugates. The retention experiment was performed according to our previous protocol.<sup>22</sup> Briefly, the cells were incubated with 5 μM Dox, NTD or C<sub>16</sub>NTD for 2 h followed by an additional 2 h incubation in drug-free medium. For quantitative evaluation, the cells were washed once with fresh medium, trypsinized and washed twice with DPBS, and the fluorescence intensity of the cells was determined using a FACScalibur flow cytometer (BD Biosciences, San Jose, CA) using the FL1 (530/30) and FL3 (670LP) channels for 5-FAM and doxorubicin, respectively. For qualitative evaluation, the cells were washed 3 times with phenol red free medium (containing 10% FBS), and imaged using an epifluorescence microscope (JENCO, Portland, OR).

**Colocalization.** KB-3-1 or KB-V1 cells were seeded onto a collagen-pretreated 8-well glass-bottom plate at 4 × 10<sup>4</sup> cells/well and incubated overnight. The cells were then incubated with fresh medium containing 5 μM Dox, NTD or C<sub>16</sub>NTD for 2 h. Thirty minutes before imaging, Hoechst 33342 (10 μg/mL, Invitrogen) and LysoTracker green (100 nM, Invitrogen) were added, and the cells were then washed twice with phenol red-free medium (Corning, Tewksbury, MA) and imaged using a Zeiss 510 confocal laser scanning fluorescent microscope (Frankfurt, Germany) in phenol red-free medium (containing 10% FBS). Blue filter (BP 420–480 nm), green filter (BP 505–

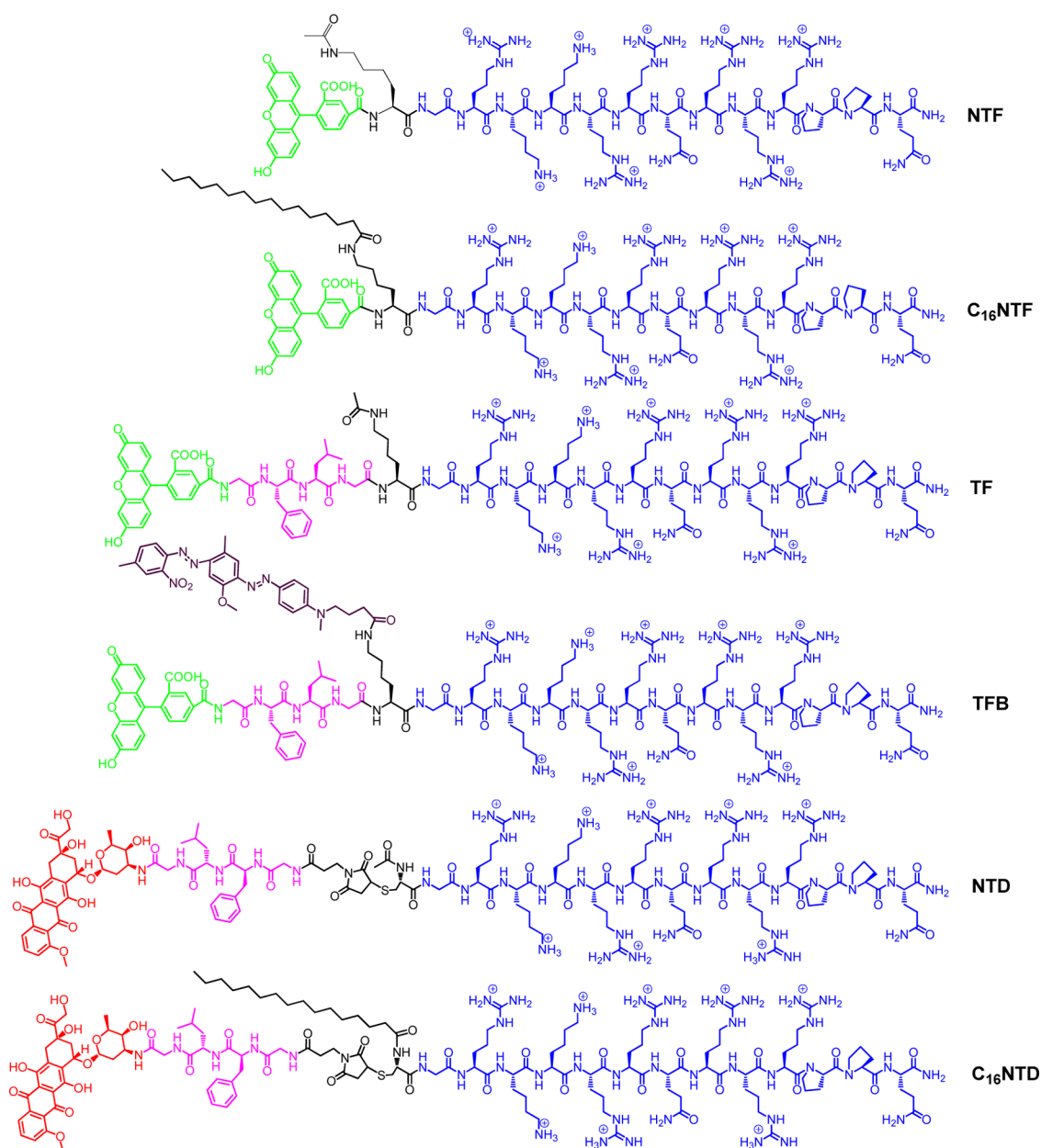


**Figure 1.** Chemical structures of the synthesized Tat conjugates (top to bottom): noncleavable Tat–5-fluorescein conjugate (NTF), palmitic acid modified noncleavable Tat–5-fluorescein conjugate ( $C_{16}$ NTF), cleavable Tat–5-fluorescein conjugate (TF), black hole quencher 1 modified cleavable Tat–5-fluorescein conjugate (TFB), cleavable Tat–doxorubicin conjugate (NTD) and palmitic acid modified cleavable Tat–doxorubicin conjugate ( $C_{16}$ NTD).

550 nm) and red filter (604–690 nm spectrum of the Meta detector) were used to recorded the fluorescence from Hoechst 33342, LysoTracker green and doxorubicin, respectively.

**Cytotoxicity.** KB-3-1 or KB-V1 cells were seeded onto a 96-well plate at  $5 \times 10^3$  cells/well and incubated overnight. The cells were first treated with fresh medium containing 5 or 15  $\mu$ M Dox, NTD,  $C_{16}$ NTD or  $C_8$ -Tat control molecule for 2 h, and further incubated with drug free medium for 46 h. Equimolar  $C_8$ -Tat was added into some wells to evaluate the effect of  $C_8$ -Tat. The cell viability was determined using the SRB method according to the manufacturer's protocol (TOX-6, Sigma, USA).

## RESULTS AND DISCUSSION

**Conjugate Design and Characterization.** In this work, the Tat peptide was chosen as the model CPP because of its wide application in drug delivery and relatively clear mechanism of cellular entry.<sup>20,25</sup> For easy molecular tracking and broad representativeness consideration, a poor cell penetrating fluorescent dye (5-fluorescein, 5-FAM) and a good cell penetrating fluorescent dye and also potent anticancer drug (doxorubicin, Dox) were chosen to conjugate to the Tat peptide. When the release of free drug is necessary, an enzymatically cleavable tetrapeptide linker, GFLG, was introduced between the drug and Tat peptide. This linker has been reported to be specifically responsive to a lysosomal enzyme, cathepsin B (CatB).<sup>37–40</sup> Palmitic acid was chosen for Tat modification because of its less crystalline nature at body



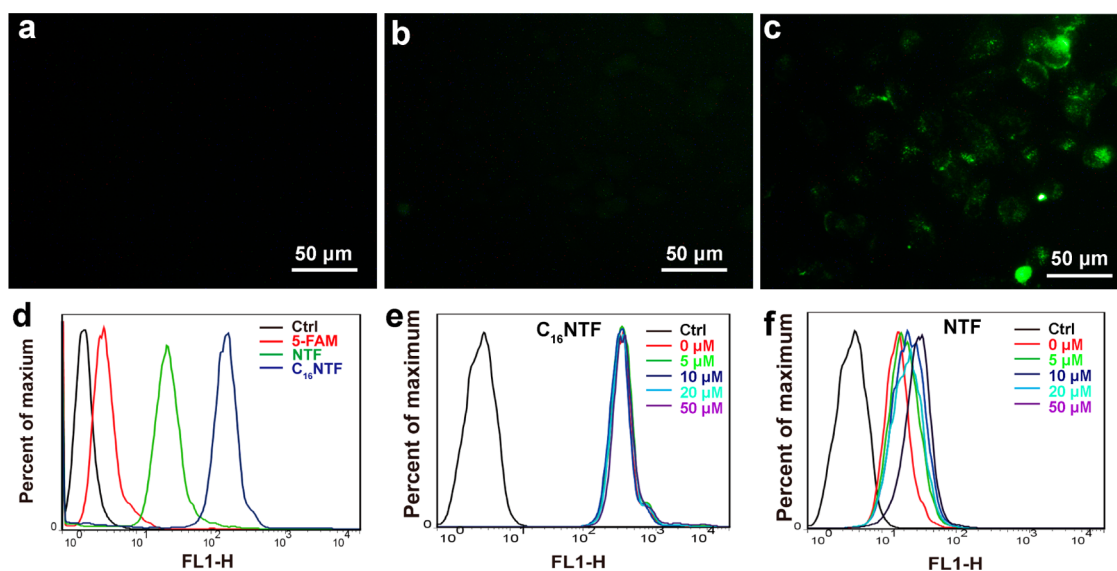


**Figure 2.** Cellular uptake of 5-FAM, NTF and  $C_{16}$ NTF by MCF-7 cells. Epifluorescent images of MCF-7 cells (post-wash with DPBS) after 2 h incubation with 5  $\mu$ M free 5-FAM (a), NTF (b) and  $C_{16}$ NTF (c). Quantitative comparison of endocytosed free 5-FAM, NTF and  $C_{16}$ NTF by MCF-7 cells after 2 h incubation with 5  $\mu$ M molecules and trypsin treatment (removes nonendocytosed conjugates) using flow cytometry at FL-1 channel (d). Quantitative comparison of endocytosed  $C_{16}$ NTF (e) and NTF (f) by MCF-7 cells after 2 h incubation with 5  $\mu$ M molecules in the presence or absence of  $C_8$ -Tat (5, 10, 20 and 50  $\mu$ M). Both the qualitative and quantitative results show greatly improved cellular uptake after lipidation of the Tat conjugates. The cellular uptake of the conjugate cannot be inhibited by even 10 times Tat peptide.

temperature, which was shown to be important for activity of modified peptides.<sup>41</sup> Additionally, palmitoylation has been widely used to construct peptide amphiphiles to promote their self-assembling feature in aqueous environments and to achieve new bioactivities.<sup>42–45</sup>

Figure 1 lists all the studied molecules in this paper. Details of the synthesis and purification can be found in the previous reports<sup>22,26</sup> and also in the Supporting Information. The purities of the two new conjugates ( $C_{16}$ NTF and  $C_{16}$ NTD) were all above 98% according to analytical HPLC analysis (Figures S1a and S2a in the Supporting Information). The  $m/z$  of  $C_{16}$ NTF was observed to be 2442.025 Da (Figure S1b in the Supporting Information), according to the MALDI-TOF mass spectrum, in agreement with the expected exact mass of the conjugate (2241.440 Da calculated from  $C_{113}H_{184}N_{38}O_{23}$ ). However, due to the chemical instability of our synthesized Tat–doxorubicin conjugates under the MALDI-TOF operation conditions,<sup>22</sup> high resolution ESI was used instead to identify their molecular masses. The  $m/z$  of  $C_{16}$ NTD was observed to be 3127.7119 Da, according to ESI mass spectrum, in agreement with the expected exact mass of the conjugate (3126.703 Da calculated from  $C_{142}H_{227}N_{43}O_{35}S$ ).

Since the hydrophilicity and hydrophobicity balance value (represented by logarithm of partition coefficient,  $\log P$ ) can be used to predict a molecule's ability to diffuse across cell membranes,<sup>46</sup> we have calculated the partition coefficients of all the studied molecules using MarvinSketch (ver. 5.12.3, ChemAxon, Cambridge, MA) (Table S1 in the Supporting Information). Due to the hydrophilic and highly positively charged nature of Tat peptide, all the Tat conjugates were calculated to have a  $\log P$  (clogP) value lower than  $-20$  in biological relevant pH. These values are out of the typical range ( $-0.4$  to  $5.6$ ) desired for molecules to effectively cross cell membranes, suggesting that free diffusion is unlikely the dominant mechanism for these Tat conjugates to get into cells.

#### Palmitoylation Significantly Improves the Cellular Uptake of Tat–5-FAM Conjugates.

To verify whether hydrophobic modification could improve cellular uptake of Tat conjugates, the cellular uptake of NTF and  $C_{16}$ NTF was compared. The only difference between these two conjugates is the introduction of palmitic acid in  $C_{16}$ NTF. Both the 5-FAM and the palmitic acid were conjugated to Tat peptide directly through an amide bond to achieve stable conjugation in order to exclude the possibility of premature degradation. As shown in Figure 2,  $C_{16}$ NTF treated cells exhibited a great improvement in fluorescence intensity which was about 40 and 6 times the intensity of 5-FAM and NTF treated cells, respectively. This is a remarkable increase considering that palmitic acid makes up only  $\sim 10\%$  of the whole conjugate by mass. Hydrophobic modification was reported to affect the secondary structure of conjugated peptide,<sup>47–49</sup> which is important to the cell penetrating efficiency.<sup>50</sup> To evaluate whether the observed difference in cellular uptake of NTF and  $C_{16}$ NTF was linked to a change in secondary structure, we recorded the circular dichroism spectrum of each conjugate (Figure S3 in the Supporting Information). These results reveal that there is no significant difference in the conformation of the two conjugates. The slight increase in the intensity for  $C_{16}$ NTF could perhaps be a result of enhanced intermolecular interactions caused by fatty acid acylation.<sup>51</sup>

Since the cellular entry of Tat peptide is generally regarded to start with its interaction with negatively charged cell membrane components (such as heparan sulfate and phospholipids),<sup>24,25</sup> it is very likely that the palmitic acid can further enhance this interaction and the subsequent adsorption-mediated endocytosis (AME) pathway,<sup>52</sup> by inserting into the hydrophobic domain of cell membrane. In an effort to verify the AME pathway that in general cannot be directly inhibited by the presence of other absorption molecules, we performed experiments to investigate the cellular uptake of  $C_{16}$ NTF in the presence of  $C_8$ -Tat of various concentrations. As shown in

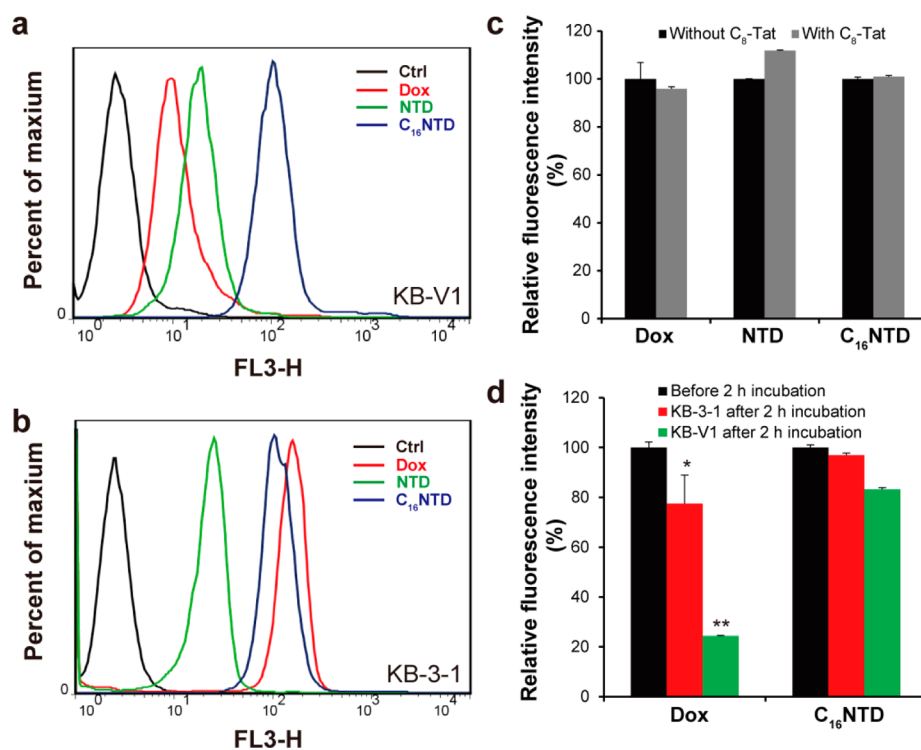


**Figure 3.** Cellular uptake of doxorubicin (Dox), NTD and C<sub>16</sub>NTD. Intracellular accumulation of free doxorubicin, NTD or C<sub>16</sub>NTD by drug-resistant cervical cancer cells KB-V1 (a) and drug-sensitive KB-3-1 cells (b) after 2 h incubation with 5  $\mu$ M molecules and trypsin treatment (removes the nonendocytosed conjugates) determined by flow cytometry at FL-3 channel. Quantitative comparison of cellular uptake of Dox, NTD or C<sub>16</sub>NTD (5  $\mu$ M) in the absence or presence of equimolar C<sub>8</sub>-Tat (5  $\mu$ M) (c). Studies on the retention ability of endocytosed Dox or C<sub>16</sub>NTD (2 h and 5  $\mu$ M) in KB-3-1 cells or KB-V1 cells after additional 2 h incubation in drug-free medium (d). \*  $p < 0.05$  compared with cells after 2 h incubation with doxorubicin. \*\*  $p < 0.01$  compared with cells after 2 h incubation with doxorubicin.

Figure 2e, the amount of C<sub>8</sub>-Tat appears to have no influence on the cellular entry of C<sub>16</sub>NTF. Even in the presence of a 10-fold excess of C<sub>8</sub>-Tat relative to C<sub>16</sub>NTF, the inhibition effect was still not observed. Similar results were also found in the cellular uptake experiments with the NTF molecule (Figure 2f). The slight difference in fluorescence intensity of cells incubated with different amount of C<sub>8</sub>-Tat is within the margin of experiment errors due to the measured low fluorescence intensity as a result of NTF's poor cellular entry. These experiments suggest that AME is the most plausible mechanism for NTF and C<sub>16</sub>NTF internalization.

**Efficient Cancer Cell Killing by Palmitoylation of Tat–Dox Conjugate Regardless of P-Glycoprotein Expression Level.** Coexistence of cancer cells with different phenotypes, termed as heterogeneity, is a big challenge in cancer chemotherapy.<sup>48,49</sup> In the case of doxorubicin, a widely used chemotherapeutic for cancer therapy, its application is greatly hampered by the development of multidrug resistance.<sup>53</sup> Conjugation of Dox to the CPPs is a facile way to increase the intracellular accumulation of Dox in multidrug resistant cells but, unfortunately, decreases accumulation of doxorubicin in sensitive cells.<sup>22,23</sup> Therefore, one type of doxorubicin derivative that can kill both sensitive and resistant cancer cells is desired for successful cancer chemotherapy. Based upon the above results from 5-FAM conjugates, C<sub>16</sub>NTD was therefore synthesized by introducing a palmitic acid at the N-terminal of the NTD conjugate (Figure 1), with the aim of increasing drug accumulation in multidrug resistant cells while retaining its efficacy in sensitive cells.

The cellular uptake of NTD and C<sub>16</sub>NTD by drug sensitive KB-3-1 cells and drug resistant KB-V1 cells was first compared using flow cytometry to confirm the effect of hydrophobic modification on cellular uptake. Consistent with our previous results,<sup>22</sup> after 2 h incubation on drug resistant cells, the intracellular accumulation of free doxorubicin (Geo mean = 11.7) was greatly inhibited by the expressed P-glycoprotein, which effluxes Dox during its diffusion across the cell membrane (Figure 3a).<sup>54</sup> The accumulation of the NTD (Geo mean = 18.2) is not affected by P-glycoprotein<sup>22</sup> and showed improvement against free doxorubicin (Figure 3a). The palmitoylation showed an exciting improvement in intracellular accumulation of Tat–Dox conjugate, evidenced by 5-time increasing when comparing C<sub>16</sub>NTD (Geo mean = 110) with NTD. It is even more exciting to find that C<sub>16</sub>NTD (Geo mean = 113) showed a comparable intracellular accumulation to free doxorubicin observed in KB-3-1 cells (Geo mean = 152), while that of NTD (Geo mean = 22.3) was much lower (Figure 3b). The difference between free doxorubicin and C<sub>16</sub>NTD is possibly due to their difference in internalization pathway, as free diffusion (Dox) is more efficient than endocytosis (Tat conjugates) in most cases.<sup>23</sup> The secondary structures of NTD and C<sub>16</sub>NTD (50  $\mu$ M in DPBS) were similar according to the CD spectra (Figure S4 in the Supporting Information), consistent with the results from the 5-FAM conjugates.

In order to investigate the role that the Tat peptide plays in the cellular uptake of doxorubicin conjugates, we conducted a series of experiments on drug resistant KB-V1 cells that are known to have a high expression level of P-glycoprotein. These experiments involved the incubation of the cells with each

individual molecule (Dox, NTD or C<sub>16</sub>NTD) in the absence and presence of equimolar C<sub>8</sub>-Tat. Figure 3c shows the flow cytometry measurement results, revealing that the intracellular accumulation of all three studied molecules is almost identical between cells with or without C<sub>8</sub>-Tat treatment. This suggests soluble Tat peptide has little impact on the P-glycoprotein's drug efflux capacity, highlighting the importance of the covalent linkage of Dox to the Tat to achieve enhanced cellular uptake.

To explore further how this covalent linkage contributes to the cellular uptake, we evaluated the retention ability of drug conjugates in both drug sensitive and resistant cell lines. These cells were incubated for 2 h with 5  $\mu$ M either Dox or C<sub>16</sub>NTD, followed by an additional 2 h incubation in drug-free medium. We found that ~20% of the internalized free doxorubicin was effluxed out of the drug sensitive KB-3-1 cells, compared to the ~80% clearance by the drug-resistant KB-V1 cells (Figure 3d). In sharp contrast, the clearance of endocytosed C<sub>16</sub>NTD from the KB-3-1 cells was almost negligible, and only ~20% loss was recorded on KB-V1 cells. These results were consistent with our previous report on the retention of NTD,<sup>22</sup> again showing that conjugation with Tat peptide presents an effective strategy to prolong the drug retention within cells. These results also demonstrate that hydrophobic modification could be used as a versatile strategy to enhance the cellular uptake of hydrophilic cargo (such as 5-FAM) or P-glycoprotein substrates (such as doxorubicin) in both drug sensitive and resistant cell lines.

Once increased intracellular accumulation was observed, we asked whether this could lead to better antitumor activity as the drug must still be released from the conjugate for it to exert an effect. Since doxorubicin is usually given as a bolus injection with a half-life of several hours,<sup>55</sup> we determined the short-term (2 h incubation) cytotoxicity of the drugs only. Consistent with the cellular uptake results, potent anticancer activity of C<sub>16</sub>NTD was observed on both cell lines regardless of P-glycoprotein level (Figure 4), while NTD showed only little activity. The mixture of Dox with equimolar Tat peptide did not display any advantageous efficacy over free Dox in killing KB-V1 cells (Figure 4b), again suggesting that soluble Tat plays little role in overcoming drug resistance. Free Dox only showed toxicity toward drug-sensitive cells after diffusion across the cell membrane,<sup>56</sup> but not on drug-resistant cells because of P-glycoprotein overexpression.<sup>54</sup> The Tat peptide showed no cytotoxicity to both the drug-sensitive and -resistant cells (Figure 4a and S5 in the Supporting Information), indicating that the peptide itself was biocompatible. These results imply that C<sub>16</sub>NTD could be a potential treatment for heterogeneous tumors containing both drug-sensitive and -resistant cells.<sup>57,58</sup>

The GFLG linker incorporated into our design is specifically sensitive to the lysosomal enzyme, CatB,<sup>59</sup> and thus doxorubicin is expected to be released within lysosomes upon their encounter with CatB.<sup>22</sup> The liberated free doxorubicin would gradually diffuse out of the lysosomes.<sup>40</sup> We therefore used confocal microscopy to monitor the subcellular localization of the endocytosed conjugates. After 2 h incubation, C<sub>16</sub>NTD showed a higher intracellular accumulation than NTD, some of which colocalized with the lysosomes (yellow dots) and some located on the cell membrane or perimembrane area in both drug-sensitive and -resistant cells (Figure 5 and Figures S6 and S7 in the Supporting Information). In sharp contrast, Dox showed high intracellular accumulation predominantly in the nuclei of sensitive cells due to its ability to readily penetrate the cell membrane and its affinity toward DNA.<sup>60</sup> No discernible Dox was observed in drug-resistant cells owing to

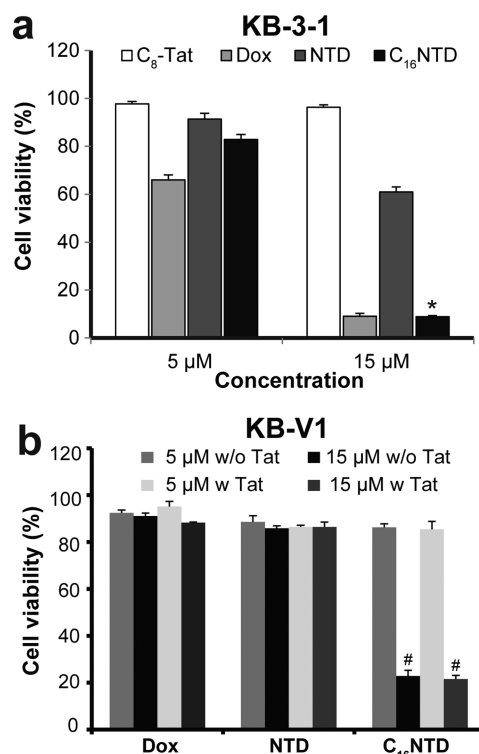


**Figure 4.** Cell viability of KB-3-1 and KB-V1 cells. Cell viability of drug-sensitive KB-3-1 (a) and drug-resistant KB-V1 (b) cells after 2 h treatment with 5 or 15  $\mu$ M free doxorubicin, NTD or C<sub>16</sub>NTD in the presence or absence of equimolar C<sub>8</sub>-Tat and a further 46 h incubation in drug-free medium. Caprylic acid modified Tat (C<sub>8</sub>-Tat) was used as control to determine the toxicity of the Tat peptide. Data is presented as mean  $\pm$  SD ( $n = 3$ ). \*  $p < 0.01$  compared with NTD; #  $p < 0.01$  compared with free doxorubicin.

drug efflux (Figure 5 and Figure S7 in the Supporting Information).<sup>54</sup> Since there is a strong electrostatic interaction between the positively charged Tat peptide and negatively charged cell membrane components,<sup>24</sup> adsorptive mediated endocytosis could be the most probable pathway for internalization as observed for a Tat-insulin conjugate<sup>61</sup> and other peptides.<sup>52,62</sup> The amount of macromolecules adsorbed on the cell membrane will likely determine the extent of intracellular accumulation.<sup>63</sup> In the presence of salts and negatively charged proteins in the cell culture medium, the electrostatic attraction will be significantly screened, and the introduction of a hydrophobic block could enhance the interaction through membrane insertion. Since both the adsorption and insertion are not cell membrane location specific and we also do not expect any self-assembled nanostructures at the studied concentrations, it is likely the bound molecules somehow concentrated to several areas before internalization.<sup>63</sup> This perhaps explains why red fluorescent dots were observed rather than continuous red staining of the cell membrane. Most of the endocytosed NTD and C<sub>16</sub>NTD were found to be colocalized with lysosomes in both KB-3-1 and KB-V1 cell (Figures 5 and S6 and S7), ensuring the release of free doxorubicin from the conjugates after endocytosis.

**Improved Imaging Contrast by BHQ1 Modification.** Intracellular enzymatic activity detection (e.g., the activity of CatB) in live cells or organisms is critical for cancer diagnosis and staging.<sup>7,64–66</sup> Due to their intracellular localization, efficient intracellular accumulation is critical to achieve high



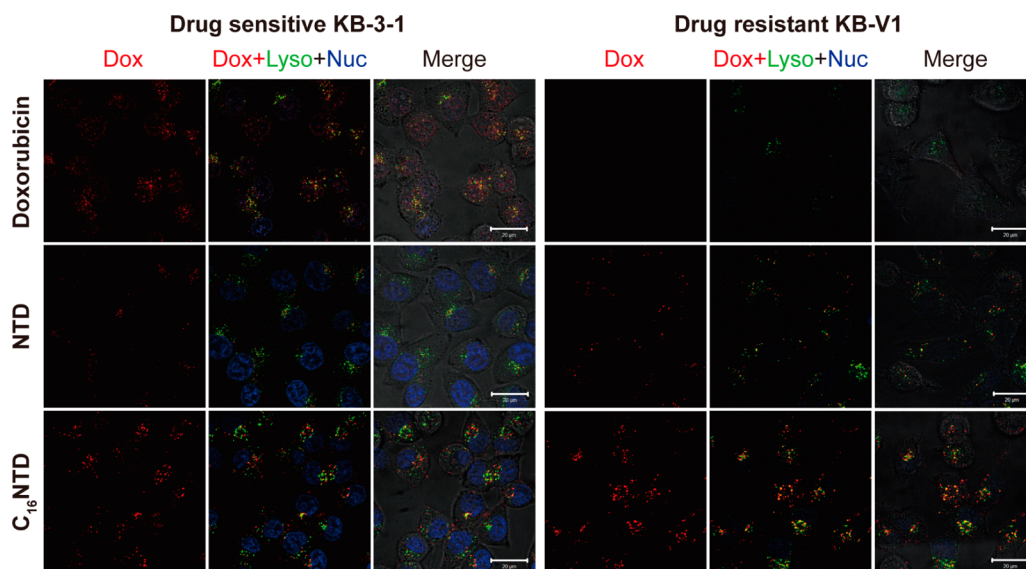


**Figure 5.** Subcellular drug localization. Subcellular colocalization of Dox, NTD or  $C_{16}$ NTD (red) in sensitive KB-3-1 and resistant KB-V1 cells with lysosome (green, LysoTracker Green) and nucleus (blue, Hoechst 33342) after 2 h drug ( $15 \mu\text{M}$ ) incubation. Scale bar:  $20 \mu\text{m}$ . The enlarged version of Figure 5 is provided in the Supporting Information as Figures S8 and S9.

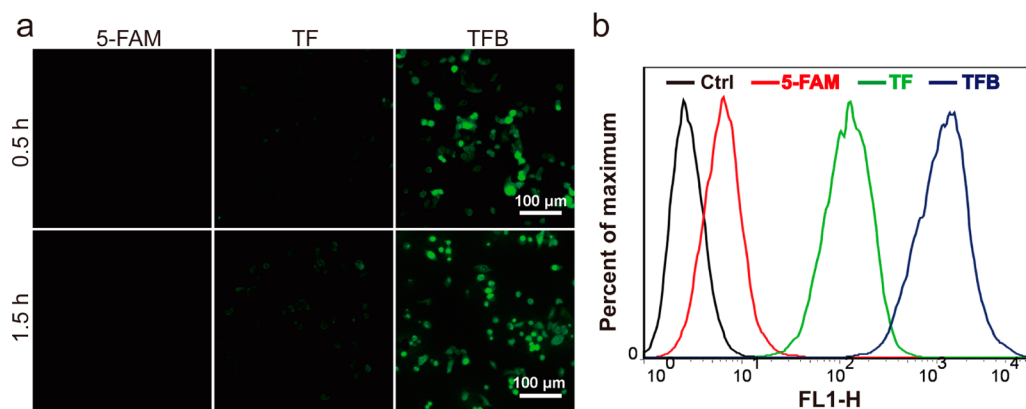


**Figure 6.** Cellular uptake of 5-FAM, TF and TFB by MCF-7 cells. Epifluorescent images of MCF-7 cells (post-wash with DPBS) after 0.5 and 2 h incubation with  $5 \mu\text{M}$  free 5-FAM, TF and TFB (a). Quantitative comparison of endocytosed free 5-FAM, TF, and TFB by MCF-7 cells after 2 h incubation with  $5 \mu\text{M}$  molecules and trypsin treatment (removes nonendocytosed conjugates) using flow cytometry at FL-1 channel (b).

contrast between intracellular signal and extracellular background noise. Since the hydrophobic modification significantly enhanced the cellular uptake of the Tat conjugate, we applied this strategy in our design of cancer imaging beacons for CatB detection.<sup>26</sup> 5-FAM was used as a reporting fluorophore, and was conjugated to Tat peptide through GFLG linker. The black hole quencher 1 (BHQ1) was chosen because of its near-perfect quenching of fluorescence from 5-FAM and the hydrophobicity required for enhanced intracellular accumulation. The successful quenching of 5-FAM fluorescence by BHQ1 in TFB was evidenced by epifluorescence images of the samples (Figure S8 in the Supporting Information), which ensures low background noise during CatB activity detection.

We first compared the fluorescence intensity of the cells treated by TF or TFB (two conjugates with similar secondary structure<sup>26</sup>) after the removal of conjugate-containing media using epifluorescence microscope (qualitative) and flow cytometry (quantitative). The fluorescence intensity of the TFB-treated cells was approximately 8 times higher than that of TF, although both conjugates showed increased cellular uptake compared with 5-FAM (about 20 times for TF and 160 times

for TFB) (Figure 6). It is noteworthy that the intracellular TFB may not be fully activated at this time point, and therefore the potential of hydrophobic modification might have been underestimated. The GFLG linker, because of its hydrophobicity, also seems to contribute to cellular uptake when comparing the relative fluorescence intensity of TF and NTF to that of 5-FAM, similar to the observed effect of the FFLIPKG sequence on octaarginine (R8).<sup>30</sup> To mimic the conditions in potential *in vivo* application, under which images would be taken in the presence of nonendocytosed beacon, the intracellular fluorescence from TFB was determined without replacing the TFB-containing media previously. A significant contrast between intra- and extracellular fluorescence was clearly observed for TFB (greater than 50% compared to control) but not for TF due to signal saturation (Figure S9 in the Supporting Information). These internalization results, consistent with those from the comparison of NTF and  $C_{16}$ NTF, clearly show that hydrophobic blocks other than fatty acids can also improve the intracellular accumulation of a Tat conjugate. In this specific case, the BHQ1 acts as dual-functional component, first as a hydrophobic block to enhance

cellular uptake and second as a quencher to 5-FAM. Taken in tandem, these two effects contribute to improved imaging contrast, a property that is critical for cancer imaging based on intracellular biomacromolecule detection.

## SUMMARY

In conclusion, our results collectively suggest the advantages of hydrophobic modification of the Tat conjugates (Figure 7).

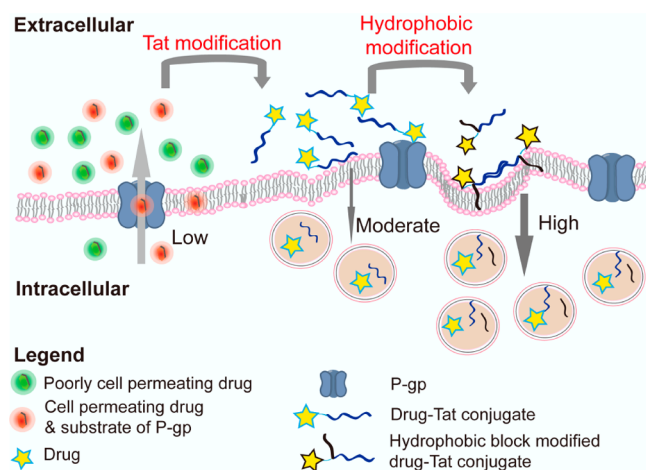


**Figure 7.** Schematic illustration of the mechanism of improved intracellular accumulation of drug through Tat and hydrophobic unit modification. The accumulation of a free drug in the cells is dependent on its logarithm of partition coefficient  $P$  ( $\log P$ ) and whether it is a substrate of efflux transporter. Conjugation of the drug to Tat peptide can improve the intracellular accumulation of drug with poor cell permeability and help the drug to bypass P-gp efflux. Further hydrophobic modification with inert fatty acid or other functional block such as quencher molecule could improve the cellular uptake of drug further and at the same time bring in new functionality to the conjugate as a molecular beacon.

First, the hydrophobic modified Tat conjugates can efficiently deliver cargoes of varying cell membrane permeability into both drug-sensitive and drug-resistant cancer cells. The cellular uptake of the hydrophobic modified Tat conjugates was comparable to that of the free form of drug with good cell membrane permeability and was greatly improved for drugs with poor cell permeability. Second, the hydrophobic modified Tat conjugates can deliver substrate of P-glycoprotein regardless of its expression level in cancer cells. Doxorubicin after conjugation with Tat peptide with a palmitoyl tail can achieve considerable intracellular accumulation and effective anticancer activity in both drug-sensitive and -resistant cells. Third, the hydrophobic unit can be a functional segment other than fatty acids, which could bring additional features to the conjugates. Hydrophobic quencher was used in our study instead of palmitic acid, and this substitution did not compromise the intracellular accumulation but rather endowed the conjugate with an additional function as a molecular beacon for probing intracellular enzyme activity in living cells. The potential of using other functional hydrophobic molecules such as hydrophobic drugs or dyes in drug-Tat conjugates could also lead to synergistic and theranostic properties.

## ASSOCIATED CONTENT

### Supporting Information

Additional characterization (HPLC and MALDI-TOF of the conjugates), CD spectra of NTF,  $C_{16}$ NTF, NTD and  $C_{16}$ NTD, darkfield and fluorescence pictures of TF and TFB solution, fluorescence image and fluorescence intensity of MCF-7 cells treated with TF or TFB, method for fluorescence determination using fluoromicroplate reader. This material is available free of charge via the Internet at <http://pubs.acs.org>.

## AUTHOR INFORMATION

### Corresponding Author

\*E-mail: [hcu6@jhu.edu](mailto:hcu6@jhu.edu). Phone: (410) 516-6878. Fax: (410) 516-5510. Johns Hopkins University, 221 Maryland Hall, 3400 North Charles Street, Baltimore, MD 21218, United States

### Notes

The authors declare no competing financial interest.

## ACKNOWLEDGMENTS

The work reported here is supported by the National Science Foundation (DMR 1255281), by the W. W. Smith Charitable Trust Fund, and by the NIH NRSA award T-32CA130840 (A.G.C.). The authors thank the Integrative Imaging Center (IIC) at the Johns Hopkins University for confocal imaging. The authors also thank Professor K. Konstantopoulos for the use of the flow cytometer, Professor M. Ostermeier for the use of the fluoromicroplate reader, Professor H. Mao for the use of the UV-vis plate reader and Professor K. Hristova for the use of the CD spectropolarimeter.

## REFERENCES

- (1) Overington, J. P.; Al-Lazikani, B.; Hopkins, A. L. Opinion - How Many Drug Targets Are There? *Nat. Rev. Drug Discovery* **2006**, *5*, 993–996.
- (2) Whitehead, K. A.; Langer, R.; Anderson, D. G. Knocking Down Barriers: Advances in SiRNA Delivery. *Nat. Rev. Drug Discovery* **2009**, *8*, 129–138.
- (3) McCormick, F. Cancer Gene Therapy: Fringe or Cutting Edge? *Nat. Rev. Cancer* **2001**, *1*, 130–141.
- (4) Lindgren, M.; Hallbrink, M.; Prochiantz, A.; Langel, U. Cell-Penetrating Peptides. *Trends Pharmacol. Sci.* **2000**, *21*, 99–103.
- (5) Leeson, P. D.; Springthorpe, B. The Influence of Drug-Like Concepts on Decision-Making in Medicinal Chemistry. *Nat. Rev. Drug Discovery* **2007**, *6*, 881–890.
- (6) Barabasi, A. L.; Gulbahce, N.; Loscalzo, J. Network Medicine: A Network-Based Approach to Human Disease. *Nat. Rev. Genet.* **2011**, *12*, 56–68.
- (7) Hanahan, D.; Weinberg, R. A. Hallmarks of Cancer: The Next Generation. *Cell* **2011**, *144*, 646–674.
- (8) Coster, H. G. L. A Quantitative Analysis of Voltage-Current Relationships of Fixed Charge Membranes and Associated Property of Punch-Through. *Biophys. J.* **1965**, *5*, 669–686.
- (9) Sharei, A.; Zoldan, J.; Adamo, A.; Sim, W. Y.; Cho, N.; Jackson, E.; Mao, S.; Schneider, S.; Han, M. J.; Lytton-Jean, A.; Basto, P. A.; Jhunjhunwala, S.; Lee, J.; Heller, D. A.; Kang, J. W.; Hartoularos, G. C.; Kim, K. S.; Anderson, D. G.; Langer, R.; Jensen, K. F. A Vector-Free Microfluidic Platform for Intracellular Delivery. *Proc. Natl. Acad. Sci. U.S.A.* **2013**, *110*, 2082–2087.
- (10) Zheng, D.; Seferos, D. S.; Giljohann, D. A.; Patel, P. C.; Mirkin, C. A. Aptamer Nano-Flares for Molecular Detection in Living Cells. *Nano Lett.* **2009**, *9*, 3258–3261.
- (11) Zheng, D.; Giljohann, D. A.; Chen, D. L.; Massich, M. D.; Wang, X. Q.; Iordanov, H.; Mirkin, C. A.; Paller, A. S. Topical Delivery of SiRNA-Based Spherical Nucleic Acid Nanoparticle Conjugates for



Gene Regulation. *Proc. Natl. Acad. Sci. U.S.A.* **2012**, *109*, 11975–11980.

(12) Gullotti, E.; Yeo, Y. Beyond the Imaging: Limitations of Cellular Uptake Study in the Evaluation of Nanoparticles. *J. Controlled Release* **2012**, *164*, 170–176.

(13) Xu, P. S.; Gullotti, E.; Tong, L.; Highley, C. B.; Errabelli, D. R.; Hasan, T.; Cheng, J. X.; Kohane, D. S.; Yeo, Y. Intracellular Drug Delivery by Poly(Lactic-Co-Glycolic Acid) Nanoparticles, Revisited. *Mol. Pharmaceutics* **2009**, *6*, 190–201.

(14) Jones, C. H.; Chen, C. K.; Jiang, M.; Fang, L.; Cheng, C.; Pfeifer, B. A. Synthesis of Cationic Poly(lactides) with Tunable Charge Densities as Nanocarriers for Effective Gene Delivery. *Mol. Pharmaceutics* **2013**, *10*, 1138–1145.

(15) Panyam, J.; Labhasetwar, V. Biodegradable Nanoparticles for Drug and Gene Delivery to Cells and Tissue. *Adv. Drug Delivery Rev.* **2003**, *55*, 329–347.

(16) Gao, Y.; Berciu, C.; Kuang, Y.; Shi, J.; Nicastro, D.; Xu, B. Probing Nanoscale Self-Assembly of Nonfluorescent Small Molecules inside Live Mammalian Cells. *ACS Nano* **2013**, *7*, 9055–9063.

(17) Yu, Y.; Chen, C. K.; Law, W. C.; Mok, J.; Zou, J.; Prasad, P. N.; Cheng, C. Well-Defined Degradable Brush Polymer-Drug Conjugates for Sustained Delivery of Paclitaxel. *Mol. Pharmaceutics* **2013**, *10*, 867–874.

(18) Koren, E.; Torchilin, V. P. Cell-Penetrating Peptides: Breaking through to the Other Side. *Trends Mol. Med.* **2012**, *18*, 385–393.

(19) Vives, E.; Brodin, P.; Lebleu, B. A Truncated Hiv-1 Tat Protein Basic Domain Rapidly Translocates through the Plasma Membrane and Accumulates in the Cell Nucleus. *J. Biol. Chem.* **1997**, *272*, 16010–16017.

(20) Brooks, H.; Lebleu, B.; Vives, E. Tat Peptide-Mediated Cellular Delivery: Back to Basics. *Adv. Drug Delivery Rev.* **2005**, *57*, 559–577.

(21) Zhang, K.; Fang, H.; Chen, Z.; Taylor, J. S.; Wooley, K. L. Shape Effects of Nanoparticles Conjugated with Cell-Penetrating Peptides (Hiv Tat Ptd) on Cho Cell Uptake. *Bioconjugate Chem.* **2008**, *19*, 1880–1887.

(22) Zhang, P.; Cheetham, A. G.; Lock, L. L.; Cui, H. Cellular Uptake and Cytotoxicity of Drug-Peptide Conjugates Regulated by Conjugation Site. *Bioconjugate Chem.* **2013**, *24*, 604–613.

(23) Aroui, S.; Ram, N.; Appaix, F.; Ronjat, M.; Kenani, A.; Pirolet, F.; De Waard, M. Maurocalcine as a Non Toxic Drug Carrier Overcomes Doxorubicin Resistance in the Cancer Cell Line Mda-Mb 231. *Pharm. Res.* **2009**, *26*, 836–845.

(24) Richard, J. P.; Melikov, K.; Brooks, H.; Prevot, P.; Lebleu, B.; Chernomordik, L. V. Cellular Uptake of Unconjugated Tat Peptide Involves Clathrin-Dependent Endocytosis and Heparan Sulfate Receptors. *J. Biol. Chem.* **2005**, *280*, 15300–15306.

(25) Mishra, A.; Lai, G. H.; Schmidt, N. W.; Sun, V. Z.; Rodriguez, A. R.; Tong, R.; Tang, L.; Cheng, J.; Deming, T. J.; Kamei, D. T.; Wong, G. C. Translocation of Hiv Tat Peptide and Analogues Induced by Multiplexed Membrane and Cytoskeletal Interactions. *Proc. Natl. Acad. Sci. U.S.A.* **2011**, *108*, 16883–16888.

(26) Lock, L. L.; Cheetham, A. G.; Zhang, P. C.; Cui, H. G. Design and Construction of Supramolecular Nanobeacons for Enzyme Detection. *ACS Nano* **2013**, *7*, 4924–4932.

(27) Zhang, P. C.; Cheetham, A. G.; Lin, Y.-A.; Cui, H. G. Self-Assembled Tat Nanofibers as Effective Drug Carrier and Transporter. *ACS Nano* **2013**, *7*, 5965–5977.

(28) Daniels, D. S.; Schepartz, A. Intrinsically Cell-Permeable Miniature Proteins Based on a Minimal Cationic PPII Motif. *J. Am. Chem. Soc.* **2007**, *129*, 14578–14579.

(29) Takayama, K.; Nakase, I.; Michiue, H.; Takeuchi, T.; Tomizawa, K.; Matsui, H.; Futaki, S. Enhanced Intracellular Delivery Using Arginine-Rich Peptides by the Addition of Penetration Accelerating Sequences (Pas). *J. Controlled Release* **2009**, *138*, 128–133.

(30) Takayama, K.; Hirose, H.; Tanaka, G.; Pujals, S.; Katayama, S.; Nakase, I.; Futaki, S. Effect of the Attachment of a Penetration Accelerating Sequence and the Influence of Hydrophobicity on Octaarginine-Mediated Intracellular Delivery. *Mol. Pharmaceutics* **2012**, *9*, 1222–1230.

(31) Ye, G.; Nam, N. H.; Kumar, A.; Saleh, A.; Shenoy, D. B.; Amiji, M. M.; Lin, X.; Sun, G.; Parang, K. Synthesis and Evaluation of Tripodal Peptide Analogues for Cellular Delivery of Phosphopeptides. *J. Med. Chem.* **2007**, *50*, 3604–3617.

(32) Nasrolahi Shirazi, A.; Oh, D.; Tiwari, R. K.; Sullivan, B.; Gupta, A.; Bothun, G. D.; Parang, K. Peptide Amphiphile Containing Arginine and Fatty Acyl Chains as Molecular Transporters. *Mol. Pharmaceutics* **2013**, *10*, 4717–4727.

(33) Missirlis, D.; Teesalu, T.; Black, M.; Tirrell, M. The Non-Peptide Part Determines the Internalization Mechanism and Intracellular Trafficking of Peptide Amphiphiles. *PLoS One* **2013**, *8*, e54611.

(34) Futaki, S.; Ohashi, W.; Suzuki, T.; Niwa, M.; Tanaka, S.; Ueda, K.; Harashima, H.; Sugiura, Y. Stearylized Arginine-Rich Peptides: A New Class of Transfection Systems. *Bioconjugate Chem.* **2001**, *12*, 1005–1011.

(35) Lehto, T.; Abes, R.; Oskolkov, N.; Suhorutsenko, J.; Copolovici, D. M.; Mager, I.; Viola, J. R.; Simonson, O. E.; Ezzat, K.; Guterstam, P.; Eriste, E.; Smith, C. I. E.; Lebleu, B.; El Andaloussi, S.; Langel, U. Delivery of Nucleic Acids with a Stearylized (Rxx)(4) Peptide Using a Non-Covalent Co-Incubation Strategy. *J. Controlled Release* **2010**, *141*, 42–51.

(36) Li, G. H.; Li, W. X.; Mumper, R. J.; Nath, A. Molecular Mechanisms in the Dramatic Enhancement of Hiv-1 Tat Transduction by Cationic Liposomes. *FASEB J.* **2012**, *26*, 2824–2834.

(37) Duncan, R.; Cable, H. C.; Lloyd, J. B.; Rejmanova, P.; Kopecek, J. Degradation of Side-Chains of N-(2-Hydroxypropyl)-Methacrylamide Copolymers by Lysosomal Thiol-Proteinases. *Biosci. Rep.* **1982**, *2*, 1041–1046.

(38) Duncan, R.; Cable, H. C.; Lloyd, J. B.; Rejmanova, P.; Kopecek, J. Polymers Containing Enzymatically Degradable Bonds. 7. Design of Oligopeptide Side-Chains in Poly[N-(2-Hydroxypropyl)-Methacrylamide] Co-Polymers to Promote Efficient Degradation by Lysosomal-Enzymes. *Makromol. Chem.* **1983**, *184*, 1997–2008.

(39) Teich, N.; Bodeker, H.; Keim, V. Cathepsin B Cleavage of the Trypsinogen Activation Peptide. *BMC Gastroenterol.* **2002**, *2*, 16.

(40) Duncan, R. Polymer Conjugates as Anticancer Nanomedicines. *Nat. Rev. Cancer* **2006**, *6*, 688–701.

(41) Chu-Kung, A. F.; Nguyen, R.; Bozzelli, K. N.; Tirrell, M. Chain Length Dependence of Antimicrobial Peptide-Fatty Acid Conjugate Activity. *J. Colloid Interface Sci.* **2010**, *345*, 160–167.

(42) Hartgerink, J. D.; Beniash, E.; Stupp, S. I. Self-Assembly and Mineralization of Peptide-Amphiphile Nanofibers. *Science* **2001**, *294*, 1684–1688.

(43) Fry, H. C.; Garcia, J. M.; Medina, M. J.; Ricoy, U. M.; Gosztola, D. J.; Nikiforov, M. P.; Palmer, L. C.; Stupp, S. I. Self-Assembly of Highly Ordered Peptide Amphiphile Metalloporphyrin Arrays. *J. Am. Chem. Soc.* **2012**, *134*, 14646–14649.

(44) Sur, S.; Matson, J. B.; Webber, M. J.; Newcomb, C. J.; Stupp, S. I. Photodynamic Control of Bioactivity in a Nanofiber Matrix. *ACS Nano* **2012**, *6*, 10776–10785.

(45) Black, M.; Trent, A.; Kostenko, Y.; Lee, J. S.; Olive, C.; Tirrell, M. Self-Assembled Peptide Amphiphile Micelles Containing a Cytotoxic T-Cell Epitope Promote a Protective Immune Response in Vivo. *Adv. Mater.* **2012**, *24*, 3845–3849.

(46) Ghose, A. K.; Viswanadhan, V. N.; Wendoloski, J. J. A Knowledge-Based Approach in Designing Combinatorial or Medicinal Chemistry Libraries for Drug Discovery. 1. A Qualitative and Quantitative Characterization of Known Drug Databases. *J. Comb. Chem.* **1999**, *1*, 55–68.

(47) Missirlis, D.; Farine, M.; Kastantin, M.; Ananthanarayanan, B.; Neumann, T.; Tirrell, M. Linker Chemistry Determines Secondary Structure of P53(14–29) in Peptide Amphiphile Micelles. *Bioconjugate Chem.* **2010**, *21*, 465–475.

(48) Missirlis, D.; Chworos, A.; Fu, C. J.; Khant, H. A.; Krogstad, D. V.; Tirrell, M. Effect of the Peptide Secondary Structure on the Peptide Amphiphile Supramolecular Structure and Interactions. *Langmuir* **2011**, *27*, 6163–6170.

(49) Mier, W.; Zitzmann, S.; Kramer, S.; Reed, J.; Knapp, E. M.; Altmann, A.; Eisenhut, M.; Haberkorn, U. Influence of Chelate Conjugation on a Newly Identified Tumor-Targeting Peptide. *J. Nucl. Med.* **2007**, *48*, 1545–1552.

(50) Duchardt, F.; Ruttekolk, I. R.; Verdurmen, W. P. R.; Lortat-Jacob, H.; Burck, J.; Hufnagel, H.; Fischer, R.; van den Heuvel, M.; Lowik, D. W. P. M.; Vuister, G. W.; Ulrich, A.; de Waard, M.; Brock, R. A Cell-Penetrating Peptide Derived from Human Lactoferrin with Conformation-Dependent Uptake Efficiency. *J. Biol. Chem.* **2009**, *284*, 36099–36108.

(51) Lin, B. F.; Missirlis, D.; Krogstad, D. V.; Tirrell, M. Structural Effects and Lipid Membrane Interactions of the Ph-Responsive Gala Peptide with Fatty Acid Acylation. *Biochemistry* **2012**, *51*, 4658–4668.

(52) Missirlis, D.; Khant, H.; Tirrell, M. Mechanisms of Peptide Amphiphile Internalization by Sjsa-1 Cells in Vitro. *Biochemistry* **2009**, *48*, 3304–3314.

(53) Persidis, A. Cancer Multidrug Resistance. *Nat. Biotechnol.* **1999**, *17*, 94–95.

(54) Akiyama, S. I.; Fojo, A.; Hanover, J. A.; Pastan, I.; Gottesman, M. M. Isolation and Genetic Characterization of Human Kb-Cell Lines Resistant to Multiple-Drugs. *Somatic Cell Mol. Genet.* **1985**, *11*, 117–126.

(55) Cao, N.; Feng, S. S. Doxorubicin Conjugated to D-Alpha-Tocopheryl Polyethylene Glycol 1000 Succinate (Tpgs): Conjugation Chemistry, Characterization, in Vitro and in Vivo Evaluation. *Biomaterials* **2008**, *29*, 3856–3865.

(56) van Lummel, M.; van Blitterswijk, W. J.; Vink, S. R.; Veldman, R. J.; van der Valk, M. A.; Schipper, D.; Dicheva, B. M.; Eggermont, A. M. M.; ten Hagen, T. L. M.; Verheij, M.; Koning, G. A. Enriching Lipid Nanovesicles with Short-Chain Glucosylceramide Improves Doxorubicin Delivery and Efficacy in Solid Tumors. *FASEB J.* **2011**, *25*, 280–289.

(57) Bhatia, S.; Frangioni, J. V.; Hoffman, R. M.; Iafrate, A. J.; Polyak, K. The Challenges Posed by Cancer Heterogeneity. *Nat. Biotechnol.* **2012**, *30*, 604–610.

(58) Bock, C.; Lengauer, T. Managing Drug Resistance in Cancer: Lessons from HIV Therapy. *Nat. Rev. Cancer* **2012**, *12*, 494–501.

(59) Turk, V.; Turk, B.; Turk, D. Lysosomal Cysteine Proteases: Facts and Opportunities. *EMBO J.* **2001**, *20*, 4629–4633.

(60) Hurley, L. H. DNA and Its Associated Processes as Targets for Cancer Therapy. *Nat. Rev. Cancer* **2002**, *2*, 188–200.

(61) Patel, E. N.; Wang, J.; Kim, K. J.; Borok, Z.; Crandall, E. D.; Shen, W. C. Conjugation with Cationic Cell-Penetrating Peptide Increases Pulmonary Absorption of Insulin. *Mol. Pharmaceutics* **2009**, *6*, 492–503.

(62) van Hell, A. J.; Fretz, M. M.; Crommelin, D. J. A.; Hennink, W. E.; Mastrobattista, E. Peptide Nanocarriers for Intracellular Delivery of Photosensitizers. *J. Controlled Release* **2010**, *141*, 347–353.

(63) Khalil, I. A.; Kogure, K.; Akita, H.; Harashima, H. Uptake Pathways and Subsequent Intracellular Trafficking in Nonviral Gene Delivery. *Pharmacol. Rev.* **2006**, *58*, 32–45.

(64) Jedeszko, C.; Sloane, B. F. Cysteine Cathepsins in Human Cancer. *Biol. Chem.* **2004**, *385*, 1017–1027.

(65) Maguire, T. M.; Shering, S. G.; Duggan, C. M.; McDermott, E. W.; O'Higgins, N. J.; Duffy, M. J. High Levels of Cathepsin B Predict Poor Outcome in Patients with Breast Cancer. *Int. J. Biol. Markers* **1998**, *13*, 139–144.

(66) Gao, Y.; Shi, J.; Yuan, D.; Xu, B. Imaging Enzyme-Triggered Self-Assembly of Small Molecules inside Live Cells. *Nat. Commun.* **2012**, *3*, 1033.